Low-Thrust Tour of the Main Belt Asteroids

Marilena Di Carlo [*], Massimiliano Vasile [†]

University of Strathclyde, Glasgow, United Kingdom

This work presents some preliminary results on the low-thrust tour of the main asteroid belt. The asteroids are visited through a series of fly-by's that minimise the total cost of the manoeuvres. The sequence of asteroids to visit and the initial orbit for the spacecraft are chosen based on the Minimum Orbit Intersection Distance (MOID) between the orbit of the asteroids and the orbit of the spacecraft. The transfers between asteroids are designed using a low-thrust analytical model that provides nearly optimal solutions with coast and thrust arcs. The mission analysis is completed with a study of the transfer of the spacecraft from the Earth to the first orbit of the tour.

Nomenclature

$\mu_\odot$	Sun's gravitational parameter
a	Semimajor axis
e	Eccentricity
r_p	Radius of perihelion
r_a	Radius of aphelion
i	Inclination
Ω	Right ascension of the ascending node
ω	Argument of the perigee
M	Mean anomaly
θ	True anomaly
P_1	Second equinoctial element
P_2	Third equinoctial element
Q_1	Fourth equinoctial element
Q_2	Fifth equinoctial element
L	True longitude
θ_{ast}^{MOID}	True anomaly of the asteroids at the critical point of the MOID
θ_{sc}^{MOID}	True anomaly of the spacecraft at the critical point of the MOID
d	Distance between objects at the critical points of the MOID
T_{ast}^{MOID}	Time when the asteroid is at θ_{ast}^{MOID}
t_0	Initial date for the main belt tour
δ	Tolerance angle for the phasing condition of the MOID
n	Total possible number of asteroid in a sequence
N	Number of selected asteroid in a sequence
$\mathcal{A}$	Sequence of asteroids
$\mathcal{T}$	Sequence of time of encounter with asteroids at θ_{ast}^{MOID}
$\mathcal{OE}$	Set of orbital elements
ΔV	Cost of the transfer
$\mathbf{LB}$	Vector of lower boundaries for the optimisation of the ΔV
$\mathbf{UB}$	Vector of upper boundaries for the optimisation of the ΔV
n_{rev}	Number of revolutions on the intermediate phasing orbit

[*] PhD Candidate, Department of Mechanical and Aerospace Engineering, University of Strathclyde, 75 Monstrose Street, G1 1XJ, Glasgow, United Kingdom.

[†] Professor, Department of Mechanical and Aerospace Engineering, University of Strathclyde, 75 Montrose Street, G1 1XJ, Glasgow, United Kingdom.

T_L	Time of launch of the spacecraft from Earth
T_M	Time of execution of the impulsive maneuver to reach the initial orbit in the main belt
$\mathbf{E}$	Vector of equinoctial elements
$\mathbf{a}_{LT}$	Low-thrust acceleration vector
ϵ	Magnitude of the low-thrust acceleration vector
α	Azimuth angle of the thrust vector in a local radial-transveral reference frame
β	Elevation angle of the thrust vector in a local radial-transveral reference frame
m	Mass of the spacecraft
$\mathbf{x}_{LT}$	Optimisable low-thrust solution vector

I. Introduction

The main belt houses the majority of the asteroids in the Solar System. It extends from 2.1 AU to 4 AU and it is estimated that several million asteroids are contained in it, ranging in size from the 972 km diameter of Ceres down to millimeters. Although larger asteroid are observable from Earth and are easy to identify, the identification and classification of smaller objects still remains an open problem. Furthermore, there is an interest in the characterisation of the larger ones to better understand their composition and evolution from the primordial stages of the Solar System till now.

However, designing a mission to characterise as many asteroids as possible in the main belt is not an easy task. The main difficulty is to identify long sequences of asteroids that can be visited in a given time and with limited ΔV. The number of known objects exceeds 100,000 and the number of possible combinations of encounter is unmanageable. The mission currently targeting objects in the main belt, Dawn,[1] is visiting only two, possibly three, proto-planets using low-thrust propulsion.

This paper presents some preliminary results on a more ambitious tour of the asteroid belt using solar electric propulsion. Two different mission scenari are considered. One starts from a shortlist of scientifically interesting targets and proceed with the analysis of all optimal sequences that are achievable with a given time limit and ΔV budget. The other leaves the choice of the scientific targets open and simply tries to find the longest sequence of objects in a given time and ΔV budgets.

In both cases the spacecraft is transferred to an elliptical orbit with perihelion at the Earth and aphelion at the main belt, to reduce both launch and ΔV requirements, each asteroid is visited with one single fly-by. A simple approach is proposed to shortlist asteroids and identify optimal sequences that can be realised with either chemical or electric propulsion. From this shortlist the best solution (longest sequence with lowest ΔV) is re-optimised with electric propulsion. A direct transcription method based on asymptotic analytical solutions to the accelerated Keplerian motion[2] is used to transcribe the optimal control problem that defines the optimal control profile of the engine. The goal is to visit the maximum possible number of asteroids in the main belt within a limited time frame. With the same transcription approach also the transfer from the Earth to the first orbit traversing the main belt is optimised. In this paper we limit our attention to transfer options that do not include swing-by's of the planets of the inner solar system, therefore the transfer from the Earth to the main belt is conceived to exploit at best the use of the launcher and the electric propulsion system. The main contribution of this paper, therefore, is in the investigation of possible sequences of fly-by's, within some constraining assumptions on time and launch mass, and their potential to be flown with an electric propulsion system.

The paper is structured as follows: it starts with a description of the proposed solution method in Section II; the results obtained are then presented in Section III and IV and Section V concludes the paper.

II. Mission Analysis

In this work two databases of objects in the main belt are considered. The first database (Database 1) is composed of 101,993 objects. The second database (Database 2) includes a selection of 424 objects of particular scientific interest. These are, among others, active objects (main belt comets, mass losing asteroids), objects of extreme sizes (both small and big) and extreme shapes, fast rotators and binaries or triples. The orbital distribution of the objects of the two database is shown in Figures 1 and 2. Note that, although the complete Database 1 contains also asteroids with perihelion at Jupiter, in this analysis we will restrict our attention to asteroids that are part of the main belt.

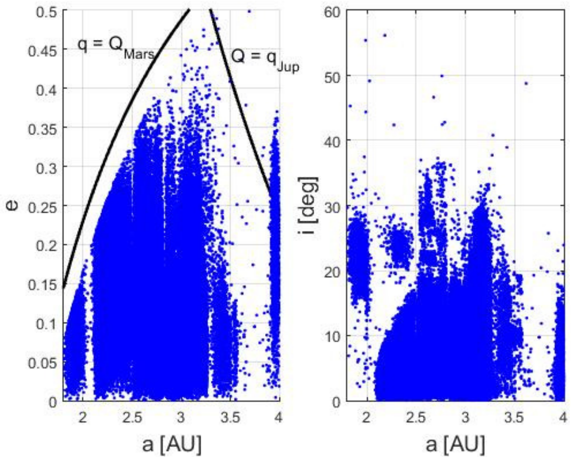

Figure 1: a-e and a-i distribution of the selected objects in the main belt for Database 1.

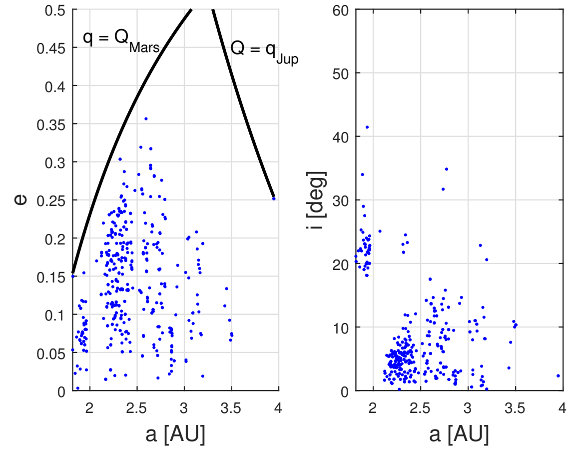

Figure 2: a-e and a-i distribution of the selected objects in the main belt for Database 2.

For both databases, the design of the mission is divided in five steps. These are briefly introduced in the following and described in more details in the next subections:

1. Analysis of the Minimum Orbit Intersection Distance (MOID) between different possible initial orbits of the spacecraft in the main belt and the orbits of all the asteroids in the database (Subsection A)
2. Analysis of the initial orbit of the spacecraft in the main belt and of the sequence of asteroids to visit using the results obtained from the computation of the MOID and a model with impulsive transfer between asteroids (Subsection B)
3. Optimisation of the time of the impulsive manuevers and of the time of the encounters with the asteroids to reduce the ΔV associated to the mission (Subsection C)
4. Study of the transfer from the Earth to the main belt (Subsection D)
5. Optimisation of the low-thrust transfer to the main belt and of the tour of the selected sequence of asteroids (Subsection E)

The tour of the main belt is assumed to start on the 01/01/2030 with a maximum duration of 5 years.

A. Minimum Orbit Intersection Distance

In order to identify the initial orbit of the spacecraft in the main belt and the sequence of asteroids to encounter, the Minimum Orbit Intersection Distance (MOID)[34] between all the asteroids in the database and different possible initial orbits of the spacecraft is computed. The MOID is defined as a measure for the geometric distance between the orbits of two objects. The computation of the MOID is realised using the Fortran code made public available online from the Department of Mathematics of the University of Pisa.[6] This computation returns, for each pair spacecraft's orbit-asteroids's orbit, the minimum, maximum and saddle points of the distance between the two orbits. These critical points are identified by the true anomalies θ_{ast}^{MOID} and θ_{sc}^{MOID} of the two objects on their orbit and by the distance between them at the critical points, d. In this study only points with $d < 0.01$ AU are considered. The computation of the MOID does not consider the positions that the asteroids and spacecraft occupy on their orbits.[5] This means that an encounter between asteroids and spacecraft can not actually take place if the two bodies are not, at the same time, at θ_{ast}^{MOID} and θ_{sc}^{MOID}. In order to check which encounters at the MOID can be realised, the following phasing analysis is applied:

- For each couple spacecraft's orbit- asteroid's orbit with $d < 0.01$ AU, the times when the asteroid is at θ_{ast}^{MOID} are computed, starting from the initial date 01/01/2030, $t_0 = 10957.5$ MJD2000. These times, that repeat at interval equal to the orbital period of the asteroids, are identified as T_{ast}^{MOID}.

- Different initial mean anomalies M_0 in the range $[0, 360)$ deg, at steps of 1 deg, are considered for the spacecraft on its orbit, with initial date t_0.
- Kepler's equation is solved to obtain the true anomaly of the spacecraft at T_{sc}^{MOID}, $\theta_{sc}(T_{ast}^{MOID})$, starting from M_0 at t_0. If the following condition is satisfied

$$|\theta_{sc}(T_{ast}^{MOID}) - \theta_{sc}^{MOID}| < \delta \tag{1}$$

then the encounters between asteroids and spacecraft, at distance d <0.01 AU is demonstrated to actually take place at time T_{ast}^{MOID}, with δ an appropriate small angle.

B. Study of possible sequences of asteroids

At the end of the process defined in the previous subsection, for each value of M_0, a list of asteroids that encounter the spacecraft at distance lower than 0.01 AU is available. The next step consists in computing the ΔV required to visit these objects, with a fly-by realised at distance equal to 0 AU, when the asteroids are at θ_{ast}^{MOID}. The Δv is estimated by connecting pairs of asteroids with Lambert's arcs.[7]

The first transfer takes place from the point defined by M_0 at t_0, on the orbit of the spacecraft, to the point defined by θ_{ast}^{MOID} for the first asteroid in the list, at time T_{ast}^{MOID}. Each subsequent transfer takes place from the previous asteroid to the next asteroid in the list, at their critical points. However, encountering each asteroid in the sequence could be too expensive in terms of ΔV. The study, therefore, tries to identify sequences that can be realised with a maximum allowable total Δv.

Sequences that satisfy the limit on the Δv are generated with a tree search on a binary tree. A generic sequence of n asteroids is identified by a vector $\mathbf{b}$ of length n composed of 0's and 1's. A 1 means that the asteroid is in the sequence (a flyby is performed) while a 0 means that the asteroid is not in the sequence (no flyby). As a results, 2^n sequences are possible, each characterised by a different number of asteroids and different values of ΔV. An enumerative approach to evaluate all the 2^n possibilities is not practical when n is large. Thus a deterministic branch and prune approach (BPA) is applied. The BPA incrementally builds a binary tree in which each level corresponds to one of the n components in $\mathbf{b}$ and each branch is a sequence. At each level each branch is divided in two subbranches one with leaf with value 1 and one with leaf with value 0. Then each partial branch is evaluated. If the ΔV associated to the partial branch exceeds a given threshold the whole branch is discarded.

After this process, for each value of M_0 on the initial orbit, the vector $\mathbf{b}$ is translated into a list of asteroids $\mathcal{A} = \{A_1, A_2, A_3, \ldots A_N\}$, with $N \leq n$ and $\Delta V < \Delta V_{max}$. The initial orbit of the spacecraft is defined through its orbital elements: $\mathcal{OE} = \{r_p, r_a, i, \Omega, \omega\}$, where r_p is the radius of perihelion, r_a is the radius of aphelion, Ω is the right ascension of the ascending node and ω is the argument of perigee and its mean anomaly M_0 at time t_0. The date of the encounters are defined as $\mathcal{T} = \{T_1, T_2, \cdots T_N\}$.

[**insert binary tree figure**]

C. Optimisation of the sequence of asteroids

The solution found at the previous step assumes that the encounters with the asteroids take place when they are at their critical true anomaly, θ_{ast}^{MOID}, starting from an initial orbit identified by $\mathcal{OE}$. A better solution might however exist and could be found by changing some of the parameters of the initial orbit $\mathcal{OE}$ or changing the date of encounter with the asteroids, that is by encountering the asteroids not exactly at θ_{ast}^{MOID}. In order to find a better solution, a global optimisation problem is solved, in which the objective is the minimisation of the ΔV for the transfer. The upper and lower bounderies for the global optimisation problem are defined by the vectors **LB** and **UB**:

$$\mathbf{LB} = [M_0 - \Delta M_0, r_p - \Delta r_p, r_a - \Delta r_a, \omega - \Delta\omega, T_1 - \Delta T_1, T_2 - \Delta T_2, \ldots T_n - \Delta T_n]^T \tag{2}$$

$$\mathbf{UB} = [M_0 + \Delta M_0, r_p + \Delta r_p, r_a + \Delta r_a, \omega + \Delta\omega, T_1 + \Delta T_1, T_2 + \Delta T_2, \ldots T_n + \Delta T_n]^T \tag{3}$$

The global search is realised using the global optimiser Multi Population Adaptive Inflationary Differential Evolution Algorithm (MP-AIDEA).[10] MP-AIDEA is a multi-population adaptive stochastic optimiser which combines Differential Evolution (DE)[8] with the working principles of Monotonic Basin Hopping Algorithm (MBH).[9]

D. Transfer to the Main Belt

This section describes the transfer strategy from the Earth to the first orbit in the main belt, identified by its orbital elements $\mathcal{OE} = \{a, e, i, \Omega, \omega, M_0, t_0\}$. The transfer is realised by injecting the spacecraft into an intermediate phasing orbit, characterised by orbital elements $\mathcal{OE}_{int} = \{a_{int}, e_{int}, i, \Omega, \omega\}$ and orbital period T_{int}. The ΔV required for the launch, ΔV_L is computed as:

$$\Delta V_L = \sqrt{2\frac{\mu_\odot}{r_\oplus} - \frac{\mu_\odot}{a_{int}}} - \sqrt{\frac{\mu_\odot}{r_\oplus}} \tag{4}$$

where $\mu_\odot$ is the Sun's planetary constant and $r_\oplus$ is the Sun-Earth distance.

The spacecraft remains on the intermediate phasing orbit for an integer number n_{rev} of revolutions. After n_{rev} revolutions, when the spacecraft is at the perihelion of the intermediate orbit, a ΔV is applied to reach the final orbit:

$$\Delta V_M = \sqrt{2\frac{\mu_\odot}{r_\oplus} - \frac{\mu_\odot}{a}} - \sqrt{2\frac{\mu_\odot}{r_\oplus} - \frac{\mu_\odot}{a_{int}}} \tag{5}$$

The spacecraft moves then for a time:

$$\Delta T = \frac{M_0 - M_p}{n} \tag{6}$$

on the orbit $\mathcal{OE}$. In the previous equation M_0 is the mean anomaly on the first orbit in the main belt at t_0, $M_p = 0$ deg is the mean anomaly at perihelion and n is the mean motion of the orbit. For every value of n_{rev}, T_{int} has to be such that at the computed time of the launch, T_L:

$$T_L = t_0 - \Delta T - n_{rev} T_{int} \tag{7}$$

the Earth is at the perihelion of the orbit $\mathcal{OE}$. This allows one to identify the value of T_{int}, and therefore the intermediate phasing orbit $\mathcal{OE}_{int}$, for every $\mathcal{OE}$ and n_{rev}.

E. Low-Thrust Optimisation

The outcome of the sequence finder and optimisation with MP-AIDEA is a sequence of transfer legs characterised by a departure heliocentric position, an end heliocentric position, a transfer time and a departure ΔV. The low-thrust optimisation process determines, for each transfer leg, an optimal control history, for the low-thrust engine, to depart from one asteroid and reach the following asteroid in the sequence at a given time. In this study, a variant of the direct analytical multiple shooting algorithm proposed by Zuiani[2] and implemented in the software code FABLE (FAst Boundary-value Low-thrust Estimator) is used. The transfer leg is split into a predefined sequence of n_{LT} finite coast and thrust arcs. Each s-th arc is represented by a vector of equinoctial parameters $\mathbf{E}_s = [a_s, P_{1,s}, P_{2,s}, Q_{1,s}, Q_{2,s}, L_s]^T$, plus, in case of thrust arc, the low-thrust acceleration components, a_r, a_t and a_h expressed in a local radial-transversal reference frame as:[2]

$$\mathbf{a}_{LT,s} = \begin{Bmatrix} a_r \\ a_t \\ a_h \end{Bmatrix}_s = \begin{Bmatrix} \epsilon_i \cos\alpha_i \cos\beta_i \\ \epsilon_i \sin\alpha_i \cos\beta_i \\ \epsilon_i \sin\beta_i \end{Bmatrix} \tag{8}$$

where α_s, β_s and ϵ_s are, respectively, the azimuth, elevation and modulus of the acceleration and $\epsilon_s = F_s/m_s$ is the ratio between thrust F_s and mass of the spacecraft m_s.

The trajectory is then analytical propagated backward from the end point and forward for the departure point (Figure 3). The motion is assumed purely Keplerian along coast arcs while thrust arcs are analytical propagated using the asymptotic expansion solutions proposed in the work of Zuiani and Vasile.[11] Each arc begins and ends at an On/Off control node, where On nodes define the switching point from a coast to a thrust arc and Off nodes define the switching point from a thrust to a coast arc (see Figure 3). Therefore, thrust arcs are defined by a set of orbital elements at an On node, E_s^{ON}, and coast arcs are defined by a set of orbital elements at an Off node, E_s^{OFF}.

For the trajectories considered in this study, the angle β is set to zero, since the transfers are all on the ecliptic plane. The azimuth angles α_s are instead optimisation variables while the modulus ϵ of the

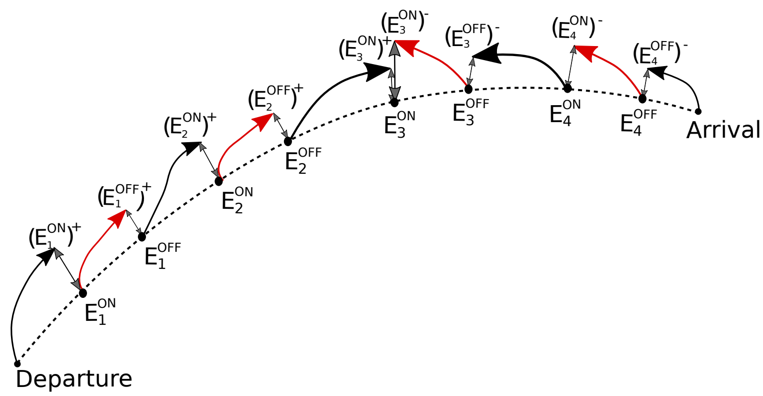

Figure 3: Segmentation of the trajectory into coast legs (black) and thrust legs (red).

acceleration depends only on the mass of the spacecraft. The mass of the spacecraft is conservatively kept constant over each transfer and updated at the end of the transfer according to the propellant mass spent to realise that transfer.

The optimisable vector for each transfer is, therefore, defined by the azimuth angles α_s, for each thrust arc, and the equinoctial elements at each On and Off point:

$$\mathbf{x}_{LT} = [\alpha_1, \mathbf{E}_1^{ON}, \mathbf{E}_1^{OFF}, \alpha_2, \mathbf{E}_2^{ON}, \mathbf{E}_2^{OFF}, \alpha_{n_{LT}}, \mathbf{E}_{n_{LT}}^{ON}, \mathbf{E}_{n_{LT}}^{OFF}]^T \tag{9}$$

where n_{LT} is the number of thrust and coast arcs.

The optimisation problem is formulated as a non-linear programming problem whose objective is the total ΔV for each transfer

$$\min_{\mathbf{x}_{LT}} \quad \Delta V = \sum_s \epsilon_s \Delta t_s \left(\mathbf{x}_{LT}\right), \tag{10}$$

where $\Delta t_s \left(\mathbf{x}_{LT}\right)$ is the time length of each thrust arc, subject to the following constraints:

$$\begin{cases} \left(\mathbf{E}_1^{ON}\right)^+ = \mathbf{E}_1^{ON} & \\ \left(\mathbf{E}_s^{OFF}\right)^+ = \mathbf{E}_s^{OFF} & s = 1, \ldots, n_{LT}/2 \\ \left(\mathbf{E}_s^{ON}\right)^- = \mathbf{E}_s^{ON} & s = n_{LT}/2+1, \ldots, n_{LT} \\ \left(\mathbf{E}_{nLT/2+1}^{ON}\right)^+ = \left(\mathbf{E}_{nLT/2+1}^{ON}\right)^- & \\ \left(\mathbf{E}_{nLT}^{OFF}\right)^- = \mathbf{E}_{nLT}^{OFF} & \\ \sum_{s=1}^{n_{LT}} \Delta t_s = ToF & \end{cases} \tag{11}$$

The plus and minus signs in the constraints equations indicate respectively the forward integration leg and the backward integration leg. The non-linear programming problem is solved using the Matlab® *fmincon-interior-point* algorithm.

III. Results Database 1

At first optimal tours are generated using Database 1. This section presents the results of the scan of all possible sequences with estimated cost lower than 1 km/s, and the low-thrust optimisation of the most promising solution.

A. Minimum Orbit Intersection Distance

The MOID is computed between all the asteroids in the database and different orbits of the spacecraft identified by the orbital elements in Table 1. The spacecraft orbits are elliptical, with perihelion at the Earth and aphelion in a given range of distances from the Sun.

Table 1: Orbital elements of the different possible initial orbits of the spacecraft used for the computation of the MOID with the asteroids of Database 1

r_p [AU]	r_a [AU]	i [deg]	Ω [deg]	ω [deg]
1	[1.86, 2.46]	0	0	[0, 360]

Figure 4 shows, for each analysed value of the aphelion r_a and for different values of ω, the number of asteroids with $d < 0.01$ AU with respect the orbit of the spacecraft. As expected, the higher the aphelion the greater the number of asteroids with $d < 0.01$ AU, as the spacecraft spends a greater part of its orbital revolution inside the main belt. This is true in the range of r_a considered in this study. The number of asteroids shown in Figure 4 does not account for the position of asteroids and spacecraft on their orbits. Once the phasing process presented in Subsection II A is applied, the number of asteroids that is possible to encounter with $d < 0.01$ is reduced. Figure 5 shows the number of asteroids which respect the condition in Equation 1, for different values of M_0 and for the value of ω giving the maximum number of asteroids with $d < 0.01$ AU; $\delta = 1$ in this case. The number of asteroids with $d < 0.01$ AU and phasing condition satisfied can be as high as 82, when $r_a = 2.46$ AU. However, only transfer with a total Δ lower than ΔV_{max} are considered. The sequence of asteroids that satisfy $\Delta V < \Delta V_{max}$ are presented in the next section.

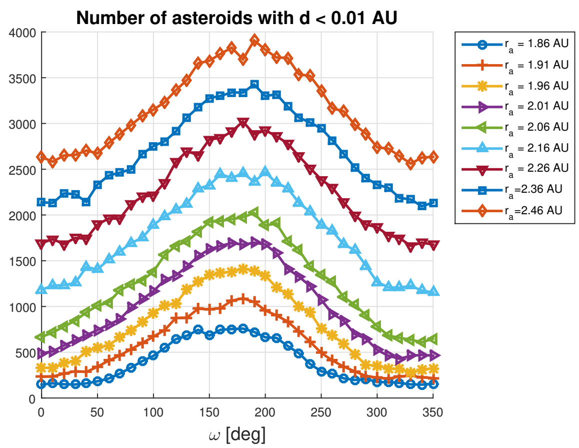

Figure 4: Number of asteroids of Database 1 with $d < 0.01$ AU for different initial orbit of the spacecraft, identified by their aphelion radius r_a.

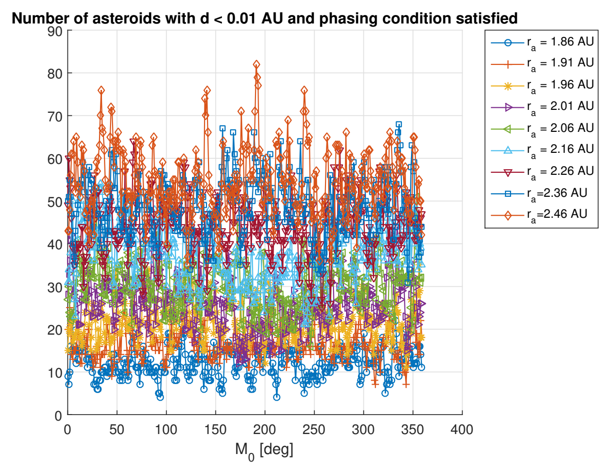

Figure 5: Number of asteroids of Database 1 with $d < 0.01$ AU and phasing condition for asteroids encounter (Equation 1) satisfied.

B. Study of the possible sequences of asteroids

Figure 6 shows the ΔV required for the tour of the asteroids, as a function of the number N of visited objects. The initial orbit of the spacecraft has $r_a = 1.86$ AU and $\omega = 180$ deg and the maximum mission cost is $\Delta V_{max} = 1$ km/s. Different values of the angle δ are considered, from $\delta = 0.1$ deg to $\delta = 1$ deg. The figures collect the results obtained for all the possible values of M_0 from 1 to 360 deg, at steps of 1 deg and for each value of N only the first 1000 best solution (the ones with lower ΔV) are shown.

Results from figure 6 show that higher values of δ allows one to find solutions with a longer list of asteroids, while still satisfying the condition $\Delta V < \Delta V_{max}$. Figure 7 shows the relation between ΔV and number of visited asteroids for orbits with different values of r_a, as defined in Table 1, and different value of δ. The value of ω for each orbit is the one that allows to visit the maximum possible number of asteroids for that r_a. As r_a increases, the maximum number of asteroids that it is possible to visit increases (from 8 for $r_a = 1.86$ AU to 11 for $r_a = 2.46$ AU)and the ΔV associated to a given number of asteroids N decreases.

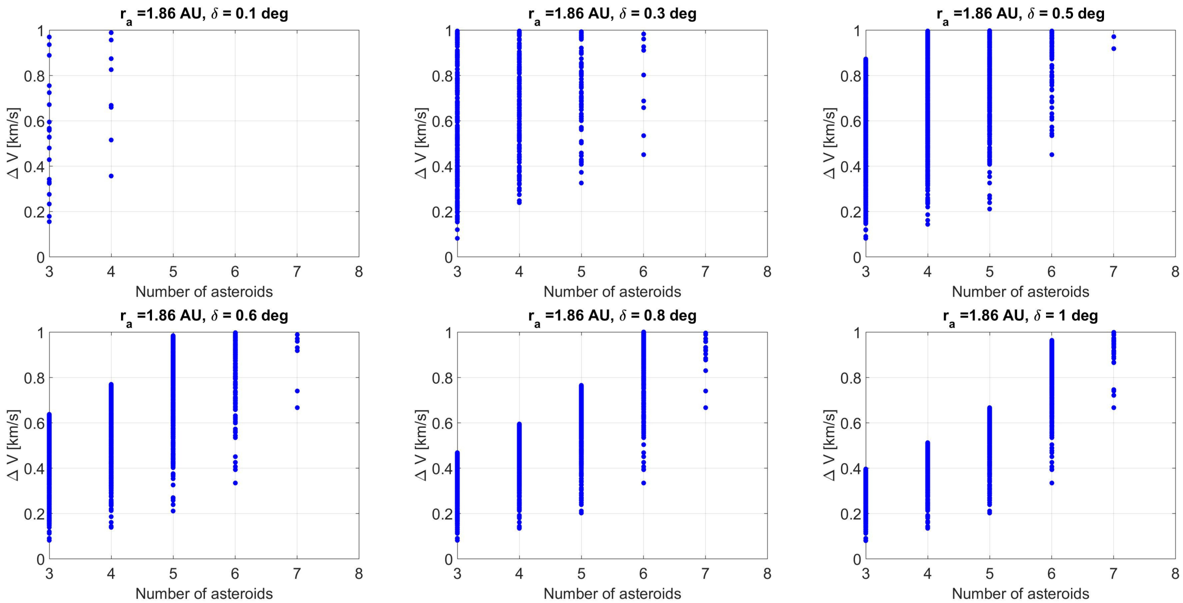

Figure 6: Relation between ΔV and number of visited asteroids for orbit with $r_a = 1.86$ AU and different values of δ.

C. Optimisation of the sequence of asteroids

For each one of the orbits in Figure 7, the solutions with maximum number of visited asteroids and lowest ΔV are further optimised using MP-AIDEA. The lower and upper boundaries **LB** and **UB** used for the optimisation with MP-AIDEA are defined by Equations 2 and 3 and the values reported in Table 2. Δr_p, Δr_a and $\Delta\omega$ are given as a function of the nominal values, r_p, r_a and ω. Each optimised result is obtained after 25 runs of MP-AIDEA, in order to obtain statistically significant results. The number of function evaluations for each run is 50,000.

Table 2: Parameters for the definition of **UB** and **LB**

ΔM_0 [deg]	Δr_p	Δr_a	$\Delta\omega$	ΔT_i [days]
1	0.01 r_{p0}	0.01 r_{a0}	0.01 ω	10

The results obtained are shown in Table 3, where also r_a and ω, the number of asteroids visited N and the ΔV of the best solution considered (maximum N, lower ΔV) are reported. The reduction in the cost of the tour, from ΔV to ΔV_{opt}, is more than 50% in some cases.

The solution selected for the low-thrust transfer optimisation is the one characterised by initial orbit with aphelion radius $r_a = 2.26$ AU, $N = 11$ and $\Delta V_{opt} = 0.5293$ km/s. Details of this tour are given in Table 4 and in Figure 8, where the initial orbit of the spacecraft is shown in black and the orbits of the visited asteroids are shown in blue. The names of the visited asteroids and the date of encounter are also shown. Table 4 gives the departure dates obtained before and after the optimisation with MP-AIDEA, the time of flight ToF and the ΔV for each single transfer. The associated initial orbit of the spacecraft in the main belt has orbital elements: $\mathcal{OE}_1 = \{a = 1.6296 \text{ AU}, e = 0.3859, i = 0 \text{ deg}, \Omega = 0 \text{ deg}, \omega = 179.9815 \text{ deg}, M_0 = 242.6178 \text{ deg}, t_0 = 10958.5 \text{ MJD2000}\}$

D. Transfer to the Main Belt

Two possibilities exist for the transfer from the Earth to the selected orbit $\mathcal{OE}_1$, with time of transfer shorter than 5 years. These two transfer possibilities are identified as T1 and T2 and are presented in Table 5. The corresponding orbits are shown in Figures 9 and 10. In Table 5 the times T_L and T_M when ΔV_L and ΔV_M

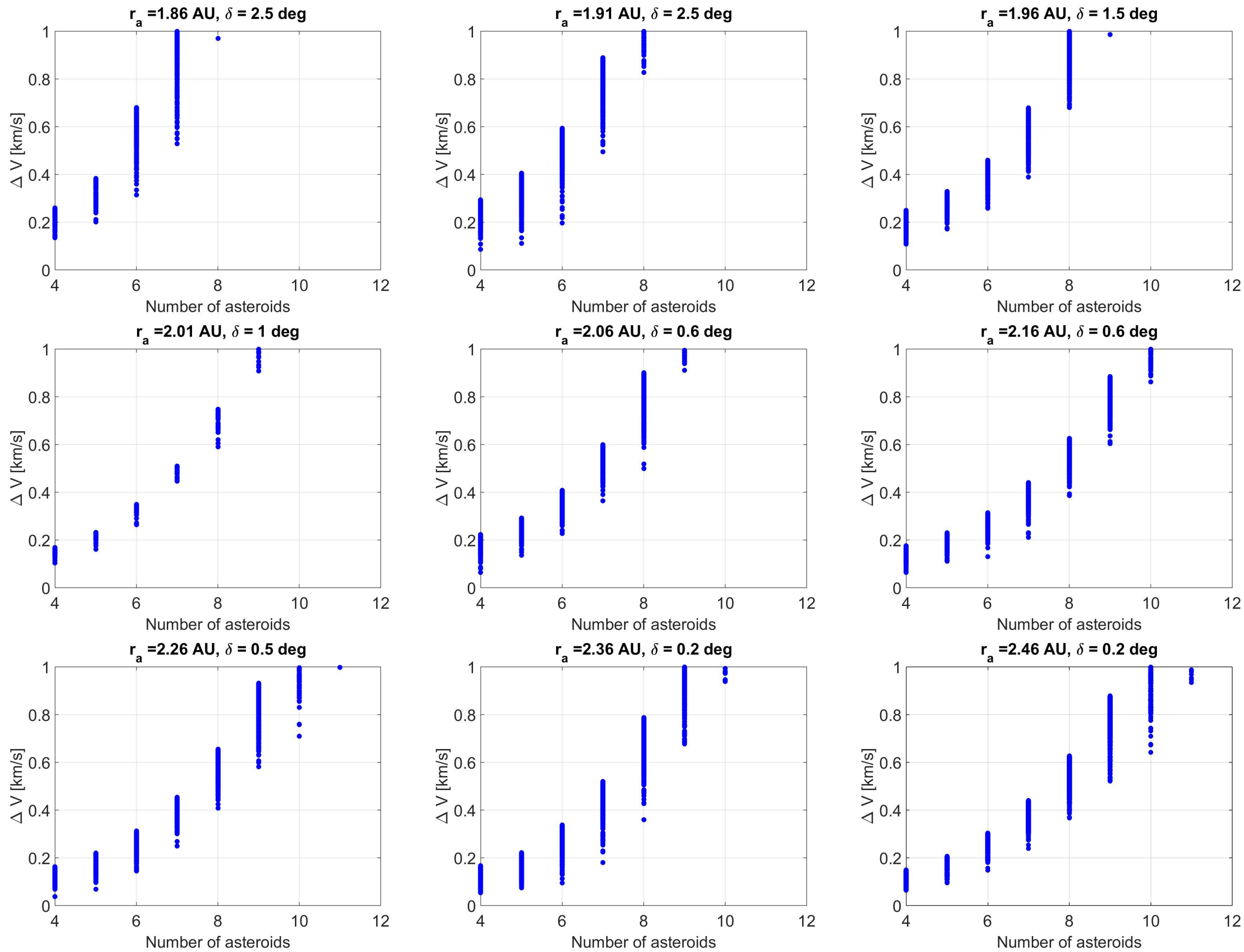

Figure 7: Relation between ΔV and number of visited asteroids for orbit with different r_a and for different values of δ.

Table 3: Optimisation of the ΔV of the longest sequence of asteroids for each value of r_a

r_a [AU]	ω [deg]	N	δ [deg]	ΔV [km/s]	ΔV_{opt} [km/s]
1.86	180	8	2.5	0.9702	0.7127
1.91	180	8	2.5	0.8269	0.4741
1.96	180	9	1.5	0.9862	0.6349
2.01	190	9	1	0.9008	0.4209
2.06	190	9	0.6	0.9107	0.5519
2.16	200	10	0.6	0.8632	0.5825
2.26	180	11	0.5	0.9982	0.5293
2.36	190	10	0.2	0.9387	0.5111
2.46	190	11	0.2	0.9342	0.6689

are applied, the corresponding ΔV and the orbital elements of the intermediate phasing orbit are given. Both these transfer orbits are considered for the low-thrust optimisation of the mission.

Table 4: Selected solution for the main belt tour for Database 1

Targeted Asteroid	Dep. Date	Optimised Dep. Date	ToF [days]	Optimised ToF [days]	ΔV [km/s]	Optimised ΔV [m/s]
2004 EL5	1/1/2030	1/1/2030	465.16	466.20	17.46	17.20
2001 SK280	11/4/2031	12/4/2031	147.04	146.23	97.35	51.23
2014 UA99	5/9/2031	5/9/2031	46.22	45.93	104.11	5.75
1994 AN15	21/10/2031	21/10/2031	152.09	152.29	120.68	19.17
2005 OA8	21/3/2032	21/3/2032	370.66	371.17	54.09	28.47
2001 SB16	27/3/2033	27/3/2033	72.72	72.60	31.88	14.94
1997 WH10	7/6/2033	8/6/2033	196.05	196.12	37.41	1.83
1997 WU26	20/12/2033	21/12/2033	131.25	131.43	120.14	115.26
2002 NO54	1/5/2034	1/5/2034	389.46	388.66	22.62	6.04
2002 JO71	25/5/2035	25/5/2035	57.33	57.65	154.36	142.04
2000 UR65	21/7/2035	22/7/2035	30.98	30.82	238.17	127.39
Tot.					998.27	529.32

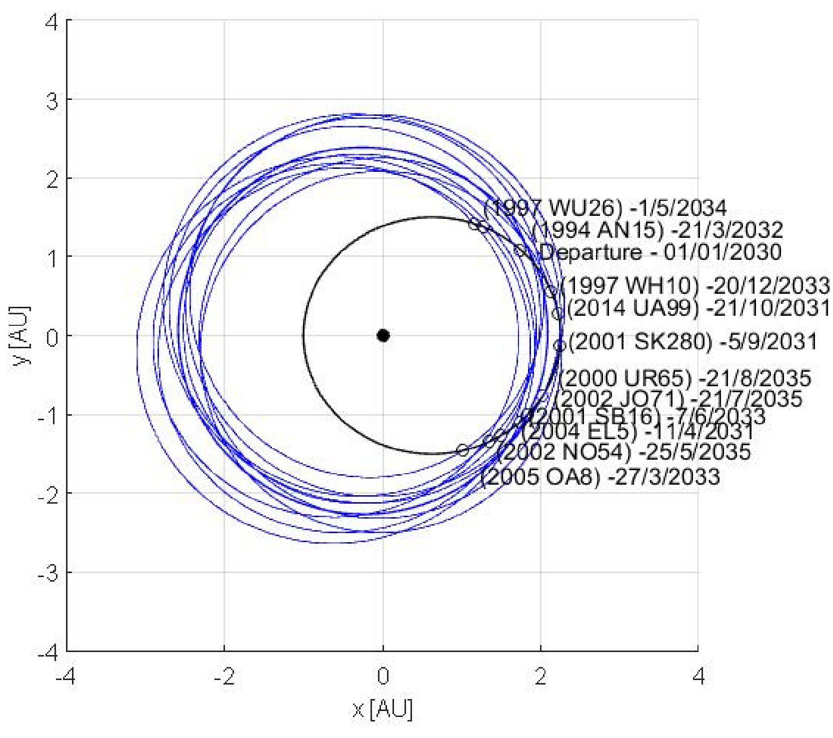

Figure 8: Selected solution for the main belt tour for Database 1

E. Low-thrust optimisation

The electrical engine conisdered in this study has a thrust magnitude equal to $F = 0.15$ N and a specific impulse $I_{sp} = 3000$ s. The initial mass of the spacecraft at launch is assumed to be $m_0 = 1000$ kg.

The ΔV required to realise the transfer to $\mathcal{OE}_1$ and the tour of the asteroids is shown in Table 6, together with the propellant consumption m_{prop} and the initial and final mass, m_0 and m_f, for the two phases of the mission (transfer to $\mathcal{OE}_1$ and tour of the asteroids). Both the possible transfer options defined in Table

Table 5: Transfers to the orbit characterised by orbital elements $\mathcal{OE}_1$ with transfer time shorter than 5 years

	T_L	ΔV_L [km/s]	a_{int} [AU]	e_{int}	n_{rev}	T_M	ΔV_M [km/s]	ΔT [days]
T1	21/03/2027	2.7531	1.2398	0.1934	1	06/08/2028	2.5319	512.06
T2	21/03/2025	4.1130	1.4189	0.2952	2	06/08/2028	1.1721	512.06

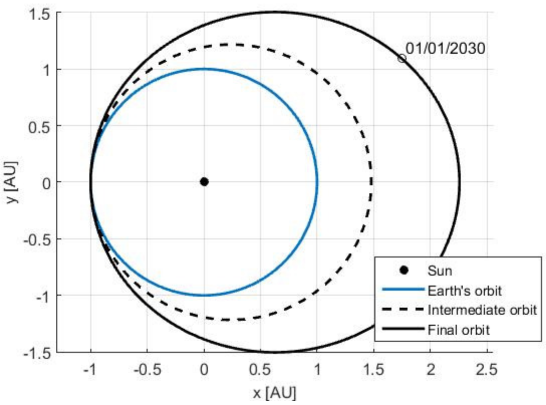

Figure 9: Orbits for transfer option T1 from Earth to orbit $\mathcal{OE}_1$

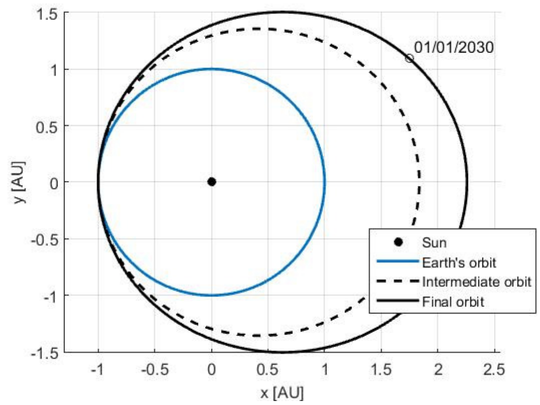

Figure 10: Orbits for transfer option T2 from Earth to orbit $\mathcal{OE}_1$.

5 are evaluated. Option T2 allows one to obtain a higher final mass at the end of the mission (906.72 kg instead than 867.49 kg) but the transfer time from Earth to $\mathcal{OE}_1$ is two years longer and the ΔV required to the launcher is higher than for option T1. The low-thrust trajectories for the transfer phases of T1 and T2 are shown in Figures 11 and 12, where the coast arcs are represented in gray and the thrust arcs in black. The low-thrust trajectory for the tour phase is shown in Figure 13 for option T1 while Figure 15 shows the variation of a and e during the low-thrust trajectory.

Table 6: ΔV and propellant consumption for the low-thrust transfer to $\mathbf{OE}_1$ and tour of Database 1

	Transfer to $\mathcal{OE}_1$				Asteroids tour			
	m_0 [kg]	ΔV [km/s]	m_{prop} [kg]	m_f [kg]	m_0 [kg]	ΔV [km/s]	m_{prop} [kg]	m_f [kg]
T1	1000	2.4425	79.72	920.28	920.28	1.7368	52.79	867.49
T2	1000	1.1316	37.76	962.24	962.24	1.7472	55.52	906.72

IV. Results Database 2

The second search for optimal tours considers only the reduced list in Database2. In this section we present the sequences and transfers calculated using the database of scientific interesting asteroids (Database2).

A. Minimum Orbit Intersection Distance

The MOID is computed between all the asteroids in the database and different orbits of the spacecraft identified by the orbital elements in Table 7.

Figure 16 shows, for the considered values of r_a, ω and i, the number of asteroids with $d < 0.01$ AU with respect to the orbit of the spacecraft. Results show that this number increases with higher r_a (as expected, since the spacecraft spends a greater part ot its orbital period inside the main belt) and with decreasing inclination. As the inclination increases a dependence on the argument of the perigee of the orbit became also evident and large regions where the number of asteroids with $d < 0.01$ AU is zero appear.

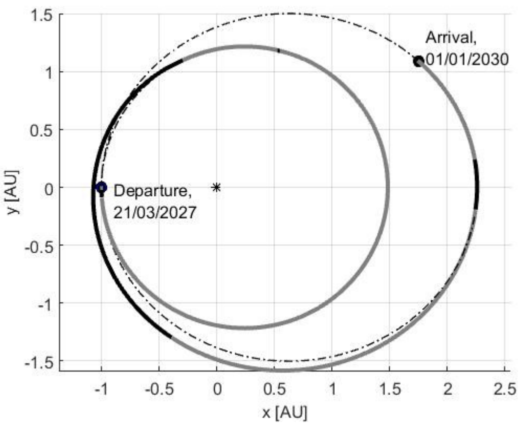

Figure 11: Low-thrust transfer trajectory to $\mathcal{OE}_1$ using option T1.

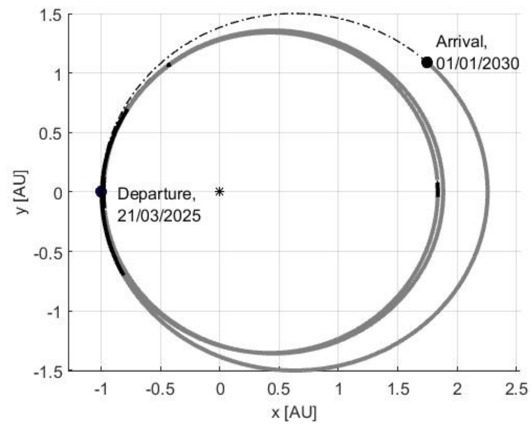

Figure 12: Low-thrust transfer trajectory to $\mathcal{OE}_1$ using option T2.

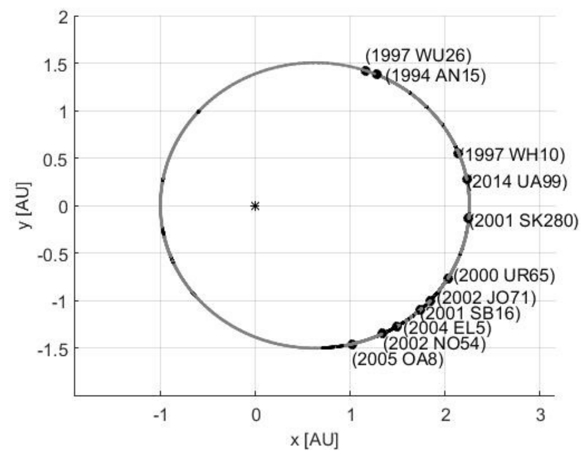

Figure 13: Low-thrust trajectory for the tour of the asteroids of Database 1.

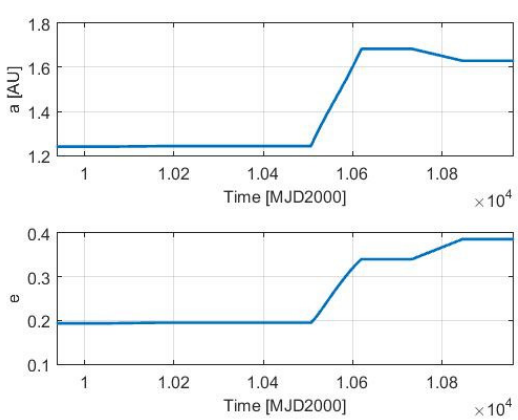

Figure 14: Variation of semimajor axis and eccentricity during the low-thrust transfer to $\mathcal{OE}_1$.

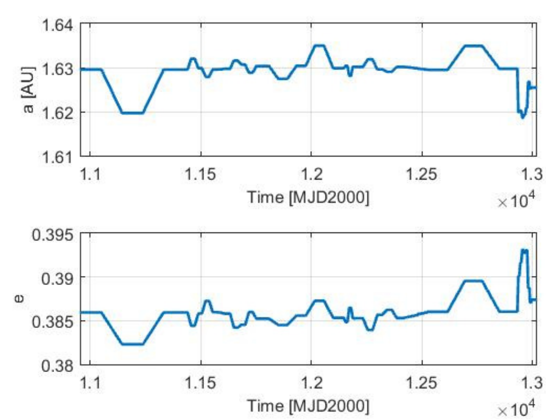

Figure 15: Variation of semimajor axis and eccentricity during low-thrust tour of the objects in Database 1.

Table 7: Orbital elements of the different possible initial orbits of the spacecraft used for the computation of the MOID with the asteroids of Database 2

r_p [AU]	r_a [AU]	i [deg]	Ω [deg]	ω [deg]
1	[1.8, 4]	[0, 30]	0	[0, 360]

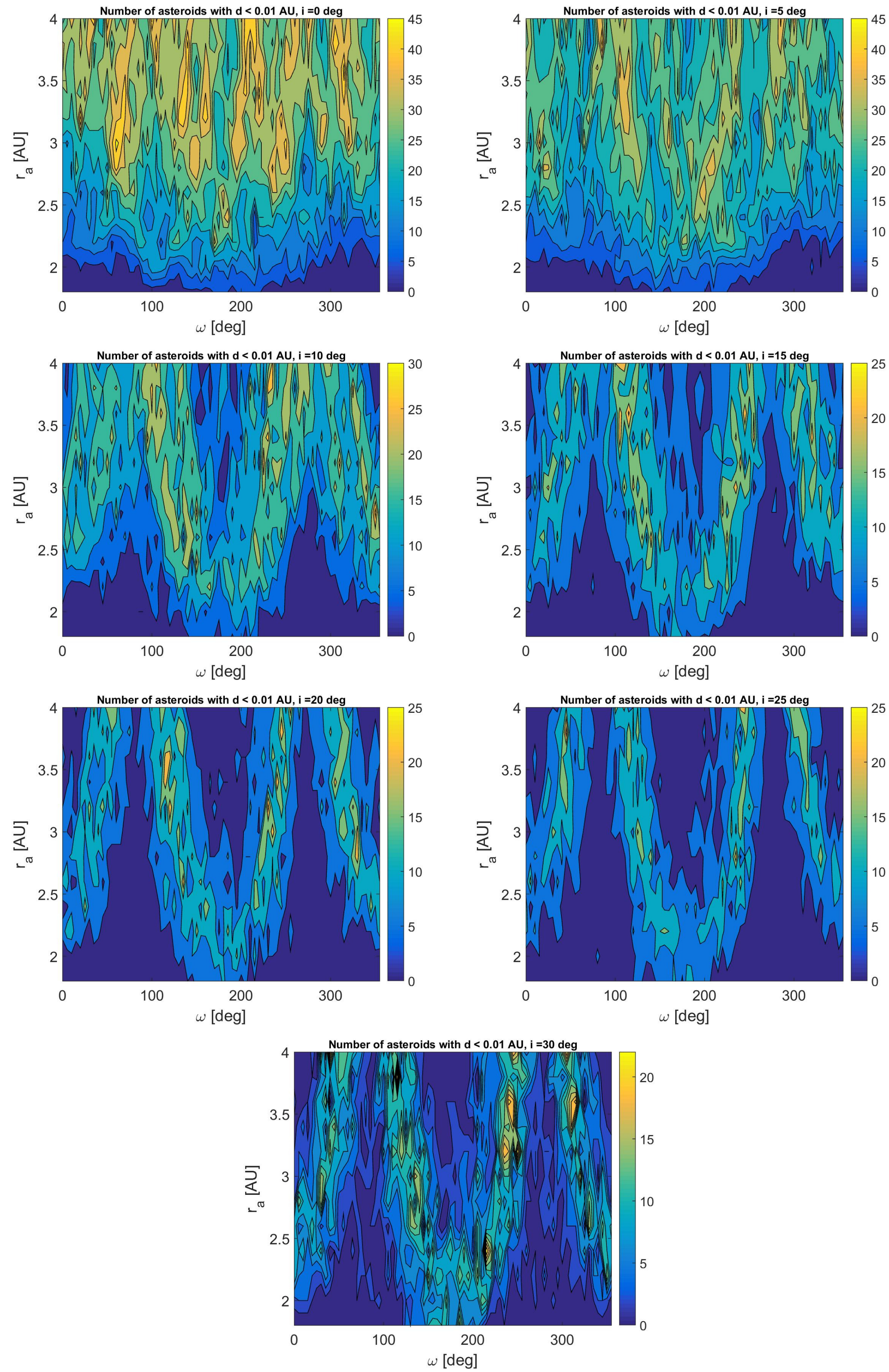

Figure 16: Number of asteroids in Database 2 with $d < 0.01$ AU for different initial orbit of the spacecraft

As in the previous analysis, the number of asteroids shown in the Figure 16 does not account for the position of asteroids and spacecraft on their orbit. Once the phasing process presented in Subsection II A is applied, the number of asteroids that is possible to encounter with $d < 0.01$ is reduced. In particular, after phasing, two orbits characterised by the highest number of encounters with the asteroids in Database 2 can be identified. The orbital elements of these two orbits (O1 and O2) are given in Table 8.

Table 8: Orbits providing the higher number of encounters with asteroids in Database 2

	a [AU]	e	i [deg]	Ω [deg]	ω [deg]
O1	2.2	0.5455	0	0	220
O2	2.3	0.5652	0	0	315

The number of possible encounters for different values of M_0 from 0 to 360 deg, for the orbits defined in Table 8, is shown in Figure 17. Results show that the maximum number of asteroids that it is possible to visit in 5 years is 8. The cost associated to the mission has to be computed to verify that it is below the limit value of $\Delta V_{max} = 1$ km/s.

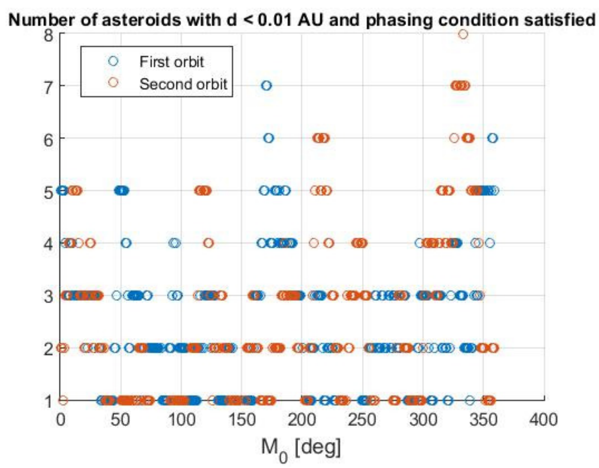

Figure 17: Number of asteroids with $d < 0.01$ and phasing condition (Equation 1) satisfied.

B. Study of the possible sequence of asteroids

Figures 18 and 19 show the ΔV required for the tour of the asteroids in Database 2, as a function of the number N of objects visited, for the two orbits defined in Table 8. The figures collect the results obtained for all the possible values of M_0 from 0 to 360 deg, at steps of 1 deg. Results show that, within the limit of $\Delta V_{max} = 1$ km/s, the maximum number of asteroids that is possible to visit is $N = 3$ for O1 and $N = 4$ for O2.

C. Optimisation of the sequence of asteroids

The best solutions in Figures 18 and 19 are optimised with MP-AIDEA. The values for the lower and upper boundaries **LB** and **UB** used for the optimisation are defined in Table 2.

The results obtained are shown in Table 3, where also the number of asteroids visited N and the ΔV of the best solution considered are reported. The reduction in the cost of the tour, from ΔV to ΔV_{opt}, is less important than in Table 3.

The solution selected for the low-thrust optimisation is the one associated to orbit 2 (O2) in Table 8, as it allows to encounters 4 rather than 3 asteroids of Database 2. Details of the transfer are given in Table 10 and in Figure 20. The initial orbit in the main belt is characterised by orbital elements: $\mathcal{OE}_2 = \{a = 2.2998 \text{ AU}, e = 0.5664, i = 0 \text{ deg}, \Omega = 0 \text{ deg}, \omega = 315.0055 \text{ deg}, M_0 = 214.4470 \text{ deg}, t_0 = 10958.5 \text{ MJD2000}\}$

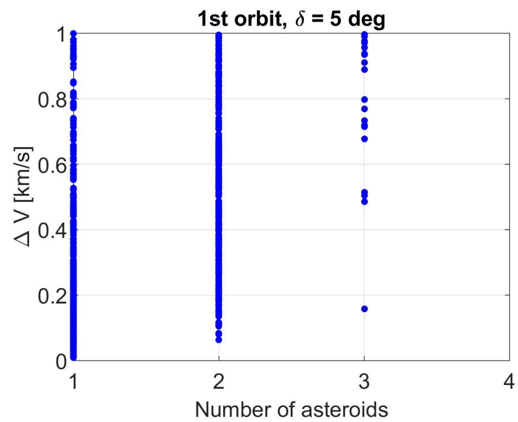

Figure 18: Relation between ΔV and number of visited asteroids for the orbit O1.

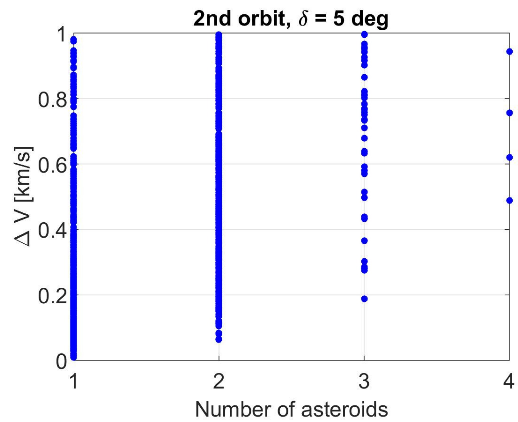

Figure 19: Relation between ΔV and number of visited asteroids for the orbit O2.

Table 9: Optimisation of the ΔV of the longest sequence of asteroids for the two orbits defined in Table 8

Orbit	N	δ [deg]	ΔV [km/s]	ΔV_{opt} [km/s]
O1	3	5	0.1580	0.1382
O2	4	5	0.4881	0.3945

Table 10: Selected solution for the main belt tour for Database 2

Targeted Asteroid	Dep. Date	Optimised Dep. Date	ToF [days]	Optimised ToF [days]	ΔV [km/s]	Optimised ΔV [m/s]
Iduna	1/1/2030	1/1/2030	294.25	297.21	80.34	64.50
Ismene	22/10/2030	25/10/2030	363.64	363.45	147.52	142.59
Urda	20/10/2031	23/10/2031	207.00	206.48	137.87	130.35
Alice	14/5/2032	17/5/2032	694.30	702.05	122.39	57.02
Tot.					488.12	394.46

D. Transfer to the Main Belt

Two possibilities exist for the transfer from the Earth to the selected orbit $\mathcal{OE}_2$, with time of transfer shorter than 5 years. The details of these options are given in Table 11 and the orbits are shown in Figure 21. Both these transfer orbits are considered for the low-thrust optimisation of the mission.

Table 11: Transfers to the orbit characterised by orbital elements $\mathcal{OE}_2$ with transfer time shorter than 5 years

	T_L	ΔV_L [km/s]	a_{int} [AU]	e_{int}	T_1 [days]	n_{rev}	T_M	ΔV_M [km/s]	T_2 [days]
T1	08/08/2026	2.4279	1.2043	0.1697	482.73	1	04/12/2027	5.0505	758.81
T2	08/08/2025	5.8288	1.7534	0.4297	847.77	1	04/12/2027	1.6496	758.81

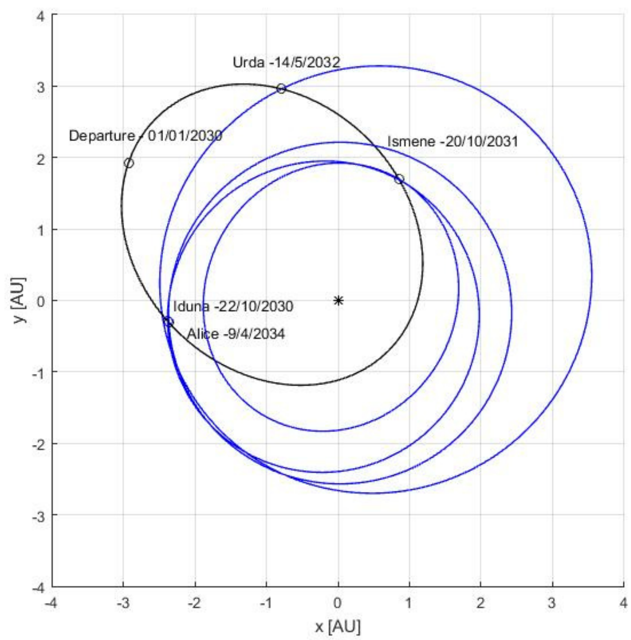

Figure 20: Selected solution for the main belt tour for Database 2

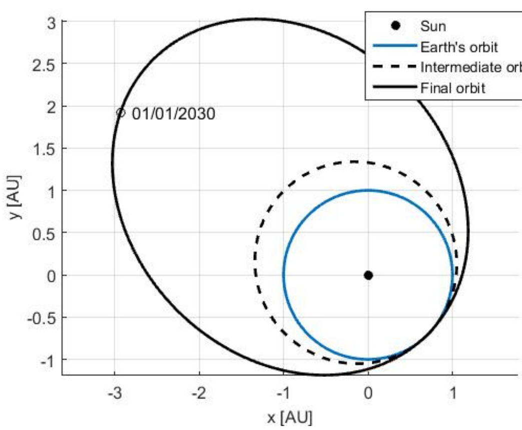

Figure 21: Transfer 1 to the orbit characterised by orbital elements $\mathcal{OE}_2$.

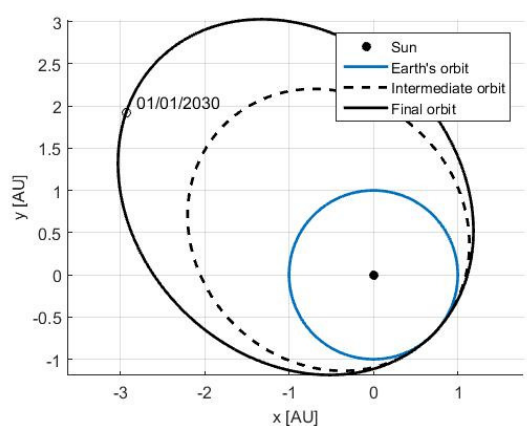

Figure 22: Transfer 2 to the orbit characterised by orbital elements $\mathcal{OE}_2$.

E. Low-thrust optimisation

The ΔV required to realise the transfer to $\mathcal{OE}_2$ and the tour of the asteroids is shown in Table 12, together with the propellant consumption m_{prop} and the initial and final mass, m_0 and m_f, for the two phases of the mission (transfer to $\mathcal{OE}_2$ and tour of the asteroids). Both the possible transfer options defined in Table 11 are considered. The low-thrust trajectories for the transfer phase T1 and T2 are shown in Figures 23 and 24, with coast arcs in gray and thrust arcs in black. The low-thrust trajectory for the tour phase corresponding to T1 is shown in Figures 25 while Figures 26 and 27 show the variation of a and e during the low-thrust trajectory. The difference in the ΔV obtained for the asteroids tour of cases T1 and T2 (0.8919 and 1.6380 km/s) is likely to be due to the convergence to different local minima when optimising the low-thrust transfer.

Table 12: ΔV and propellant consumption for the low-thrust transfer to $\mathbf{OE}_2$ and for the asteroids tour of Database 2

	Transfer to $\mathcal{OE}_2$				Asteroids tour			
	m_0 [kg]	ΔV [km/s]	m_{prop} [kg]	m_f [kg]	m_0 [kg]	ΔV [km/s]	m_{prop} [kg]	m_f [kg]
T1	1000	4.1142	130.59	869.41	869.41	0.8919	25.98	843.4318
T2	1000	1.4715	48.82	951.18	951.18	1.6380	51.55	899.6331

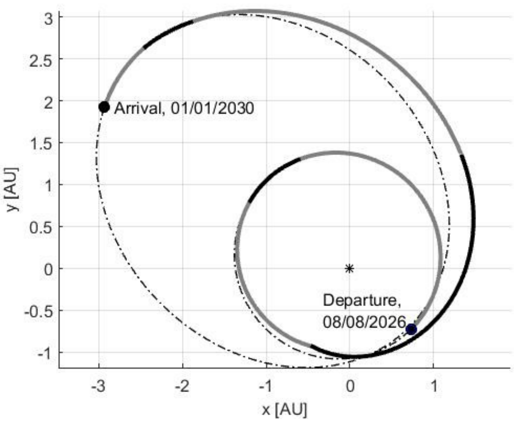

Figure 23: Low-thrust transfer trajectory to $\mathcal{OE}_2$, option T1.

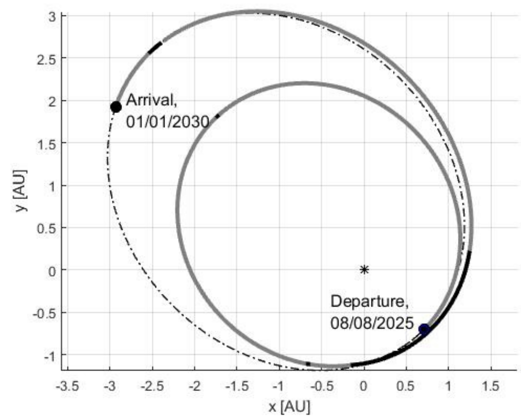

Figure 24: Low-thrust transfer trajectory to $\mathcal{OE}_2$, option T2.

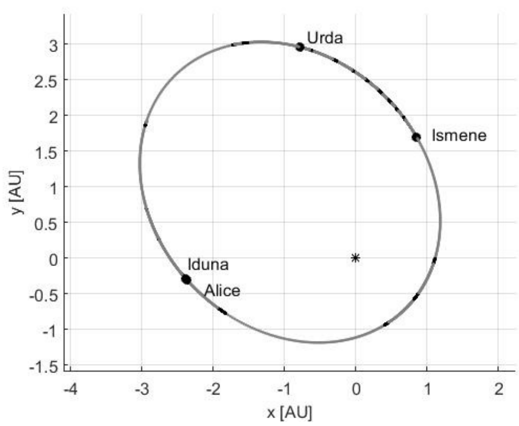

Figure 25: Low-thrust trajectory for the tour of the asteroids of Database 2

V. Conclusions

The paper presented some preliminary results for a possible low-thrust tour of the main belt. In order to limit the mission time and propellant cost it was decided to limit the analysis only to elliptical orbits with perihelion at the Earth and aphelion in a given range of distances from the Sun. The search for optimal sequences considered two different databases: one containing a large number of unsorted objects and one with a down selection of targets of particular scientific interest. This first analysis showed that, with a threshold of 1 km/s on the preliminary estimation of the ΔV, over 11 asteroids can be visited in about five years. The shortlist of scientifically interesting targets is more limited, including only four asteroids in the same time span. However, it was noted that by increasing the δ tolerance on the phasing and relaxing

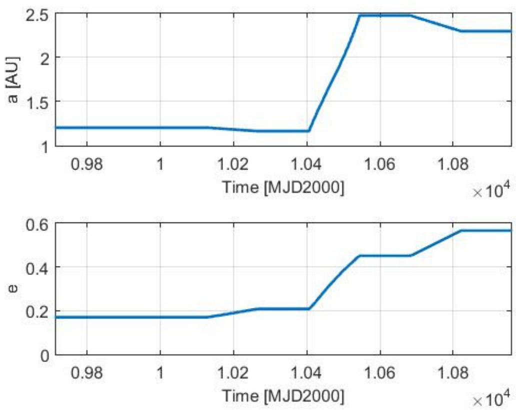

Figure 26: Variation of semimajor axis and eccentricity during the low-thrust transfer to $\mathcal{OE}_2$.

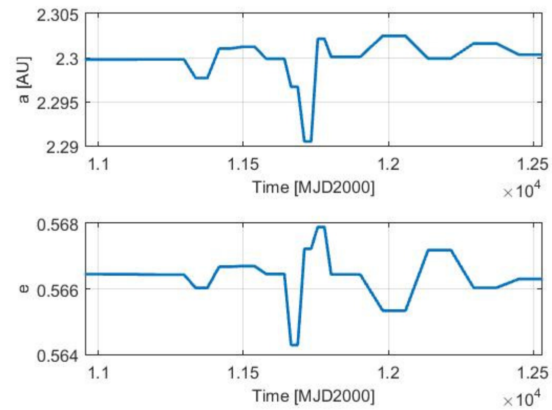

Figure 27: Variation of semimajor axis and eccentricity during the low-thrust transfer tour of the asteroids of Database 2.

the constraint on the estimated ΔV even longer sequences might be possible with an optimised ΔV that is contained below 1 km/s. Furthermore, the launch and transfer strategy in this preliminary analysis do not include any swing-by. More alternative solutions are, therefore, to be expected. This will be the object of a future study.

Acknowledgments

This research was partially funded by Airbus Defence and Space and partially by the FP7 MSCA ITN Stardust. The authors would like to thank Dr Pau Sanchez, at Cranfield University, the CASTAway team, and Mr Stephen Kemble, at Airbus DS, for their support and advice. The authors would like to thank the Institute of Engineering and Technology for the IET Travel Award to attend the Space 2016 Forum and present this work.

References

[1]Brophy, J .R., Rayman, M. D. & Pavri, B., Dawn: An ion-propelled journey to the beginning of the Solar System, 2008 IEEE Aerospace Conference, Big Sky, Montana, USA. doi: 10.1109/AERO.2008.4526264

[2]Zuiani, F., Vasile, M., Palmas, A. & Avanzini, G., Direct transcription of low-thrust trajectories with finite trajectory elements, Acta Astronautica, Vol. 72, pp. 108-120, 2012. doi: 10.1016/j.actaastro.2011.09.011

[3]Gronchi, G. F., On the stationary points of the squared distance between two ellipses with a common focus, SIAM Journal on Scientific Computing, vol. 24, p.61-80, 2002

[4]Gronchi, G. F., An algebraic method to compute the critical points of the distance function between two Keplerian orbits, Celestial Mechanics and Dynamical Astronomy, vol. 93, p.295-329, 2005

[5]Bonanno, C., An analytical approximation for the MOID and its consequences, Astronomy and Astrophysics, vol. 360, p.411-416, 2000

[6]http://adams.dm.unipi.it/ gronchi/HOMEPAGE/research.html, Accessed May 2016.

[7]Vallado, D., Fundamentals of Astrodynamics and Applications, Space Technology Library, 2007

[8]Price, K., Storn, R.M. & Lampinen, J.A., Differential evolution: a practical approach to global optimization, Springer Science and Business Media, 2006. doi: 10.1007/3-540-31306-0.

[9]Wales, D.J. & Doye, J.P., Global optimization by basin-hopping and the lowest energy structures of Lennard-Jones clusters containing up to 110 atoms, The Journal of Physical Chemistry A, 101(28), pp. 5111-5116, 1997. doi: 10.1021/jp970984n

[10]Di Carlo, M., Vasile, M., Minisci, E., Multi-Population Adaptive Inflationary Differential Evolution Algorithm, 2015 IEEE Congress on Evolutionary Computation, 25-28 May 2015, Sendai, Japan

[11]Zuiani, F. & Vasile, M., Extended analytical formulas for the perturbed Keplerian motion under a constant control acceleration, Celestial Mechanics and Dynamical Astronomy, Vol. 121, Issue 3, pp. 275-300, 2015. doi: 10.1007/s10569-014-9600-5

[12]Yam, C.H. and Longuski, J.M., Reduced parameterization for optimization of low-thrust gravity-assist trajectories: case studies, AIAA/AAS Astrodynamics Specialist Conference and Exhibit, Keystone, CO, 2006.